

Ariadne: A Controllable Framework for Probing and Extending VLM Reasoning Boundaries

Minghe Shen¹, Zhuo Zhi¹, Chonghan Liu², Shuo Xing³, Zhengzhong Tu³, Che Liu^{†4}

¹University College London ²University of California, Los Angeles ³Texas A&M University ⁴Imperial College London

[†]Corresponding author

While Vision-Language Models (VLMs) post-trained with Reinforcement Learning (RL) show impressive general reasoning, their evaluation is often confined to language-dominant tasks (e.g., math). This raises a critical question: can RL post-training truly extend the *inherent capability boundary* of a base VLM, particularly for visual-centric spatial tasks where it initially fails? To investigate this, we introduce **Ariadne**, a framework utilizing synthetic mazes for multi-step spatial reasoning where task difficulty (e.g., path length, turns) is precisely controlled. We leverage this controllable environment to train VLMs using Reinforcement Learning with Verified Rewards (RLVR) in a difficulty-aware curriculum. Surprisingly, post-RLVR training, the VLM achieves over **50%** accuracy on a problem set where the base model scored **0%**, demonstrating that our approach expands the model’s initial capability boundary. To assess real-world viability, we evaluate out-of-distribution (OOD) generalization on practical benchmarks. Despite training only on synthetic maze samples, Ariadne achieves significant zero-shot improvements, averaging 16% on MapBench (e.g., museum navigation) and 24% on ReasonMap (subway transfer tasks). These results confirm that our method not only broadens the model’s fundamental limits but also enhances its generalization to real-world spatial reasoning. We acknowledge our study is limited to the post-training phase, given the opaqueness of pre-training data, and hope our research motivates further work on specialized, capability-extending alignment.

Date: November 4, 2025

Correspondence: che.liu21@imperial.ac.uk

1 Introduction

Reinforcement Learning (RL) has played a pivotal role in advancing the reasoning capabilities of large language models (LLMs) [1, 2]. Recent work, such as DeepSeek-R1 [3], demonstrated that Group Relative Policy Optimization (GRPO), trained with Reinforcement Learning with Verified Rewards (RLVR) and without a separate reward model, can effectively enhance complex reasoning abilities [3, 4]. Extending this paradigm to the vision-language domain [5, 6, 7], Vision-Language Models (VLMs) show strong reasoning potential after RL post-training. However, their evaluation remains largely confined to language-dominant tasks such as mathematics. A key question thus arises: *Can RLVR extend the inherent capability boundary of VLMs, particularly in visual-centric spatial reasoning?*

To create a controllable scenario for evaluation, we select visual-spatial reasoning tasks such as path-finding mazes, which are well-suited for this study because they provide deterministic ground-truth paths for verifiable rewards [8, 9]. Moreover, maze complexity can be precisely adjusted through parameters such as path length and number of turns, enabling systematic probing of model reasoning behavior. To this end, we introduce **Ariadne**, a fully controllable framework designed to probe and extend VLM reasoning boundaries. Ariadne enables fine-grained control over maze complexity while maintaining clear difficulty definitions and verifiable rewards. This design allows transparent analysis of a base VLM’s capability boundary and how RLVR extends it. Furthermore, we transfer RLVR-trained VLMs to real-world benchmarks for zero-shot evaluation, exploring whether reasoning learned from synthetic mazes generalizes to practical tasks.

The main contributions of this work are summarized as follows:

- We propose **Ariadne**, a controllable framework to explore VLM reasoning boundaries post-RLVR training using purely synthetic maze tasks.
- Ariadne-trained VLMs achieve over 50% accuracy on maze problems where the base model scored 0%, demonstrating a clear expansion of the initial capability boundary.
- Beyond synthetic tasks, Ariadne achieves notable zero-shot improvements on real-world benchmarks (*MapBench* [10] and *ReasonMap* [11]), confirming that RLVR can broaden VLM reasoning across both in-domain and out-of-distribution settings.

2 Related Work

2.1 Reasoning in VLMs

VLMs have achieved substantial progress on tasks such as Visual Question Answering (VQA) and image captioning [12, 13, 14]. To strengthen reasoning capabilities, prior work has explored Chain of Thought (CoT) prompting [15] and the construction of Supervised Fine-Tuning (SFT) datasets enriched with step-level rationales [14]. While these strategies enhance reasoning to some extent, they fall short of capturing human-like cognitive processes such as questioning and self-verification, and their effectiveness diminishes on complex reasoning tasks. Recent models such as DeepSeek-R1 [4] attempt to address this gap by combining cold-start initialization with RL, thereby acquiring higher-quality multimodal CoT reasoning and achieving state-of-the-art results on challenging visual reasoning benchmarks.

2.2 Reasoning with RL

Despite the advances in VLMs, spatial and multi-step reasoning, particularly in navigation and spatial understanding, remains a key challenge. To overcome this limitation, researchers have increasingly adopted RL-based approaches. Ji et al. applied GRPO with structured CoT supervision to spatial VQA and navigation tasks, showing that verifiable, rule-based rewards can significantly improve reasoning robustness [16]. Similarly, CoT-VLA extended CoT reasoning to vision–language–action models, where explicit intermediate reasoning steps yielded strong gains in robotic navigation [17]. In synthetic navigation domains, Mirowski et al. enhanced RL training with auxiliary tasks such as depth prediction and loop-closure detection, enabling efficient traversal of complex 3D mazes [9].

While these approaches have shown effectiveness, most rely on large-scale synthetic data or are narrowly tailored to specific architectures. Open questions remain regarding how VLMs adapt their reasoning strategies when systematically exposed to increasing task complexity and to what extent such improvements generalize beyond synthetic environments [11, 10].

In this work, we introduce a controllable training framework, Ariadne, for exploring the visual reasoning boundary of VLMs. Ariadne enables precise manipulation of problem complexity while maintaining consistent logical structures and verifiable rewards, allowing both targeted capability enhancement and systematic analysis of generalization and failure modes. Finally, through evaluation on real-world map navigation datasets, we demonstrate that reasoning gains achieved in synthetic maze environments can effectively transfer to practical out-of-domain scenarios.

3 Methodology

3.1 Preliminaries of GRPO

Recent advancements in enhancing the reasoning capabilities of vision-language models (VLMs) have demonstrated that RL is a powerful training strategy [4]. In this study, we adopt GRPO as our learning framework. GRPO operates by directly comparing groups of candidate responses, thereby eliminating the need for a separate critic model.

During training, GRPO generates a set of candidate outputs o_1, o_2, \dots, o_G for a given question q drawn from the dataset \mathcal{D} using the old policy $\pi_{\theta_{\text{old}}}$. Each candidate response o_i is then evaluated using a reward

function $R(o_i, q)$, yielding a reward r_i . To assess the relative quality of the responses within the group, GRPO normalizes the rewards by computing their mean and standard deviation. The advantage A_i for each response is then calculated as:

$$A_i = \frac{r_i - \text{mean}\{r_1, r_2, \dots, r_G\}}{\text{std}\{r_1, r_2, \dots, r_G\}} \quad (1)$$

GRPO optimizes the policy model π_θ by maximizing the following objective:

$$\mathcal{J}_{\text{GRPO}}(\theta) = \mathbb{E}_{q \sim \mathcal{D}, \{o_i\}_{i=1}^G \sim \pi_{\theta_{\text{old}}}(O|q)} \left[\frac{1}{G} \sum_{i=1}^G \min \left(\frac{\pi_\theta(o_i|q)}{\pi_{\theta_{\text{old}}}(o_i|q)}, \text{clip} \left(\frac{\pi_\theta(o_i|q)}{\pi_{\theta_{\text{old}}}(o_i|q)}, 1 - \epsilon, 1 + \epsilon \right) \right) \right] \quad (2)$$

where ϵ is the clipping hyper-parameter.

3.2 Reward Function

We design a reward function to measure the stepwise correctness of model-generated answers relative to a ground truth reference. The function (Algorithm 1) assigns proportional rewards for both fully correct and partially correct answers, using the number of reasoning *turns* as a scaling factor.

Step Extraction. Each model completion is first standardized via a format extraction function to ensure consistent formatting. Reasoning steps are represented as a sequence of *moves* embedded in the format:

<|step content|>.

A count turns function extracts these moves using a regular expression, returning both the ordered list of moves and the number of *turns*, defined as the count of transitions between consecutive distinct moves.

Reward Calculation. Let $R = [r_1, r_2, \dots, r_m]$ be the predicted move sequence and $A = [a_1, a_2, \dots, a_n]$ be the ground truth. The reward is computed as:

$$\text{reward} = \begin{cases} 0.2 \times m \times \text{turns}(A), & \text{if } R = A, \\ 0.1 \times k \times \text{turns}(A_{1:k}), & \text{if only first } k \text{ moves match.} \end{cases}$$

This ensures:

- Full matches receive maximum proportional reward.
- Partial matches are rewarded according to the matching prefix length k .
- The conversational or reasoning complexity, measured by *turns*, scales the reward.

Algorithm 1 Correctness Reward Function

```

1: function CORRECTNESS_REWARD(completions, answers)
2:   rewards  $\leftarrow$  []
3:   for all  $r, a$  in (completions, answers) do
4:      $r\_moves, r\_turns \leftarrow$  count_turns( $r$ )
5:      $a\_moves, a\_turns \leftarrow$  count_turns( $a$ )
6:     if  $r\_moves = a\_moves$  then
7:       reward  $\leftarrow$  len( $a\_moves$ )  $\times$  0.2  $\times$   $a\_turns$ 
8:     else
9:        $k \leftarrow$  length of matching prefix( $r\_moves, a\_moves$ )
10:       $k\_turns \leftarrow$  count_turns(first  $k$  moves of  $a$ )
11:      reward  $\leftarrow$   $k \times$  0.1  $\times$   $k\_turns$ 
12:     end if
13:     rewards.append(reward)
14:   end for
15:   return rewards
16: end function

```

4 Experiments

4.1 Experimental Settings

4.1.1 Dataset

To control the difficulty of training samples, we design the distribution of maze step counts $s \in \{1, 2, 3, 4, 5\}$ based on an inverted Gaussian-like distribution centered at step count 3. Specifically, the sampling probability for each step count is defined as:

$$P(s) \propto 1 - \exp\left(-\frac{(s - \mu)^2}{2\sigma^2}\right), \quad (3)$$

where $\mu = 3$ is set as the midpoint of the step range, and $\sigma = 2$ is manually chosen to control the spread. This design ensures that both simpler (1–2 steps) and more complex trajectories (4–5 steps) are sampled more frequently. The resulting empirical distribution approximates {21%, 18%, 16%, 18%, 21%}, respectively.

We posit that frequent exposure to simple cases, where each step involves selecting from up to four possible directions but is often constrained by walls blocking some paths, helps the model acquire stable and generalizable low-level navigation patterns by learning to effectively choose feasible moves in a limited and structured action space. At the same time, challenging cases (with longer trajectories) drive the model to learn global spatial reasoning and coherent path planning over multiple steps. Additionally, a test set is constructed from AlphaMaze by evenly sampling across the number of moves.

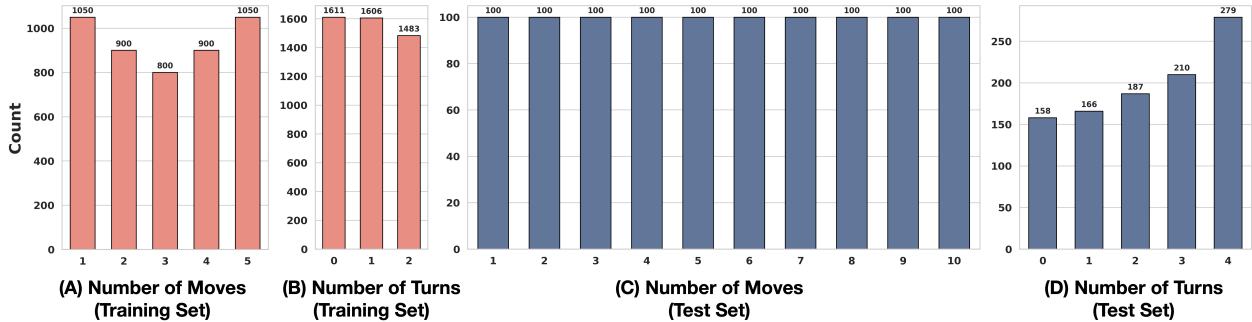


Figure 1 (A) Step-length distribution in the AlphaMaze [8] training set, where the number of moves $s \in \{1, 2, 3, 4, 5\}$ is sampled according to an inverted Gaussian-like distribution centered at $s = 3$, ensuring higher frequencies for both simple and complex cases. (B) Distribution of directional turns in the training set under the same controlled sampling scheme. (C) Step-length distribution in the AlphaMaze [8] testing set, constructed via uniform sampling. (D) Distribution of directional turns in the testing set under the same controlled sampling scheme.

Figure 1 illustrates the statistical properties of navigation trajectories in both the training and testing sets. Panels (A) and (C) depict the distributions of step lengths, reflecting the frequency of various movement distances during training and testing episodes, respectively. Panels (B) and (D) show the distributions of directional turns, emphasizing the complexity of orientation changes involved in path-finding across the two sets.

During training, the number of moves is limited to **1–5** and the number of turns to **0–2**. In the testing phase, these constraints are relaxed to **1–10** moves and **0–4** turns, enabling evaluation of generalizability on cases of higher difficulty beyond those seen in the training set.

4.1.2 Implementation

We adopt Qwen2.5-VL-7B-Instruct [18] as our base policy VLM. In our Ariadne framework, Qwen2.5-VL-7B-Instruct is trained with RLVR using 4,700 samples from the AlphaMaze [8] dataset with the GRPO algorithm, targeting enhanced reasoning performance in maze navigation tasks. Our reward function combines three factors: answer accuracy, answer format, and reasoning format, emphasizing correctness while maintaining response clarity and structure. Training is conducted on 8 NVIDIA A100 (40GB) GPUs with a learning rate of $1e-6$ for one iteration, using a batch size of 1 per device and 16 gradient accumulation steps, totaling

722,000 steps. We apply a warmup ratio of 0.05, and for each prompt, 8 candidate responses are sampled using a temperature of 1.0. The clipping hyperparameter ϵ is set to 0.2 by default. During evaluation on AlphaMaze and MapBench, each prompt is tested with 8 independent rollout samples at a temperature of 1.0, and the final results are averaged across these runs to ensure validity and reliability.

4.1.3 Prompt

The following prompt defines a navigation assistant designed for visual path-finding in AlphaMaze. Given a maze image with a green starting cell (“O”) and a red target cell (“T”), the assistant must infer a valid path that passes exclusively through open cells while avoiding black walls.

System Prompt for AlphaMaze

You are a navigation assistant to solve visual path-finding tasks.
Your goal is to infer a valid path from a visually marked starting point (green cell labeled ‘O’) to a visually marked target (red cell labeled ‘T’) by analyzing the maze image.
Rules:
- The maze is composed of open paths and impassable black walls.
- Movement is only allowed through open paths, not through walls.
- You can move one step at a time in the four cardinal directions: `<|up|>`, `<|down|>`, `<|left|>`, `<|right|>`.
Output Format:
Think through each step inside `<think>` and `</think>` tags.
At each step:
1. Describe your current position based on visual layout and structure (e.g., “in a corridor”, “facing a wall”, “at a crossroad”, “turning a corner”).
2. Decide the next move, and explain your reasoning.
3. Move and continue the path.
After your full reasoning, output only the final movement sequence using the allowed tokens:
`<|up|><|down|><|left|><|right|>`

4.2 Benchmarks and Metrics

As illustrated in Figure 2, we utilize MapBench [10] and ReasonMap [11] to evaluate the visual reasoning capabilities of VLMs. MapBench consists of human-readable map navigation tasks curated from challenging real-world scenarios [10]. ReasonMap [11] evaluates multiple-step visual reasoning using high-resolution transit maps from global metropolitan areas such as Los Angeles, Toronto, and Beijing. It adopts a two-tier evaluation protocol comprising short and long questions to measure both the correctness of the answers (via accuracy) and the quality of the answers (via a proposed map score that reflects the feasibility and efficiency of the route).

In MapBench [10], the models generate a navigation response given a map image and a query specifying the starting and ending landmarks. The final performance is defined as the ratio between the length of the model-generated path and the length of the shortest path of the ground-truth, which serves as a metric of the efficiency of the route.

For ReasonMap [11], accuracy is evaluated through a comprehensive validation process that verifies the departure and arrival stops, matches each segment’s route name with the map metadata, confirms the validity of intermediate stops, and ensures transfer consistency. An answer is considered correct only if all criteria are satisfied. For short questions, the map score emphasizes route and endpoint consistency, while for long questions it additionally accounts for the number of stops and the correctness of specific via stops. Both accuracy and map score are weighted according to question and map difficulty, enabling difficulty-aware evaluation.



Figure 2 Illustrative examples from our two controlled benchmarks for path-finding evaluation. **MapBench** (left) features human-readable, outdoor navigation tasks derived from challenging real-world scenarios (e.g., mall navigation), designed to assess naturalistic instruction-following and local decision-making. **ReasonMap** (right) uses high-resolution transit maps from global metropolitan systems (e.g., Los Angeles, Toronto, Beijing), with a two-tier evaluation (short vs. long questions) to probe both fine-grained visual comprehension and global route planning.

4.3 Main Results

4.3.1 RLVR Enables VLMs to Break Reasoning Boundaries

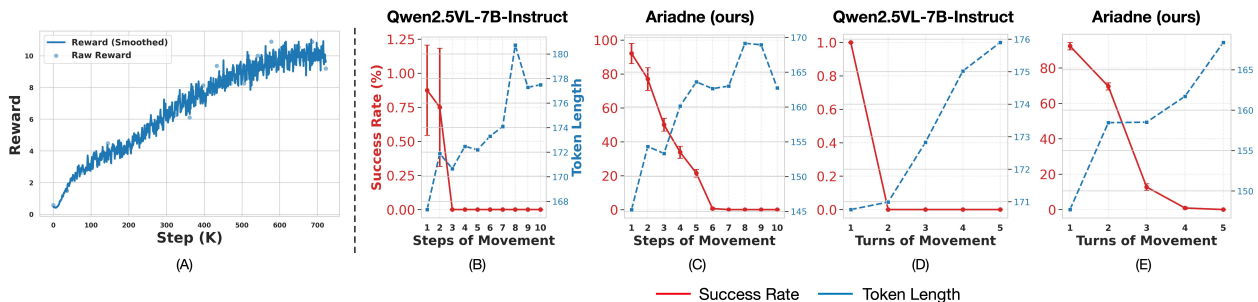


Figure 3 Training reward dynamics and evaluation of path-following ability. **(A)** Reward curve during GRPO training, showing steady improvement in rewards and stable learning progress. **(B, D)** For Qwen2.5-VL-7B-Instruct, the success rate rapidly collapses to zero (at cases with 3 movement steps or 3 turns), while token length increases, suggesting that the VLM generates longer but unsuccessful trajectories. **(C, E)** In contrast, our Ariadne framework demonstrates a remarkable improvement in success rates at the base VLM boundary, raising performance from 0% to 50% on 3-step cases and from 0% to over 10% on 3-turn cases. Token length grows moderately, and the collapse point shifts from 3 to 5, reflecting that after RLVR training, the VLM succeeds on tasks where the base model consistently failed, indicating an extended reasoning boundary.

Figure 3 presents the reward trajectory during GRPO training on AlphaMaze, along with quantitative evaluations on the test set. Across all evaluated movement step ranges, Ariadne shows a consistent advantage over its base model, Qwen2.5-VL-7B-Instruct. For Qwen2.5-VL-7B-Instruct, we perform eight rollouts to confirm model stability and observe that performance drops to zero when the path requires three movement steps or three turns, which we define as the model’s reasoning boundary. After RLVR training, Ariadne’s success rate rises to over 50% on 3 step cases and over 10% on 3 turn cases, and the collapse point shifts from 3 to 5, indicating that RLVR effectively extends the model’s reasoning boundary to more complex path configurations.

The qualitative examples in Figure 4 further illustrate these results. Successful trajectories generally occur in mazes with simple layouts and moderate detour requirements, allowing coherent path following. In contrast, failure cases are often associated with local structural complexity, dense turns, narrow corridors, and elongated

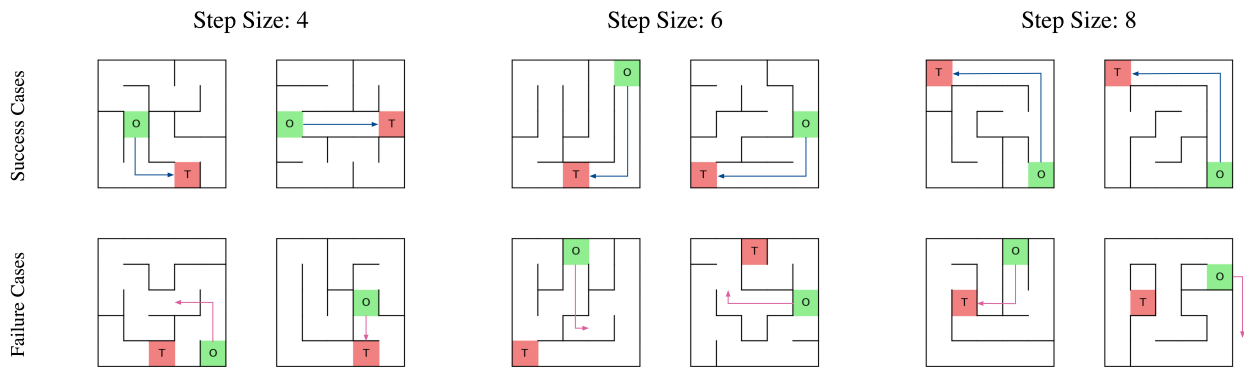


Figure 4 Representative success (top row) and failure (bottom row) cases from the AlphaMaze test set under controlled step sizes (4, 6, 8). Success cases generally correspond to smoother layouts with limited detour requirements, enabling coherent long-range navigation. Failure cases, by contrast, arise in locally complex structures characterized by dense turns, narrow passages, and elongated detours, which challenge the model’s ability to maintain global path consistency.

detours that make it difficult for the model to maintain consistent global navigation.

4.3.2 RLVR Extends VLM Reasoning to Real-world Tasks

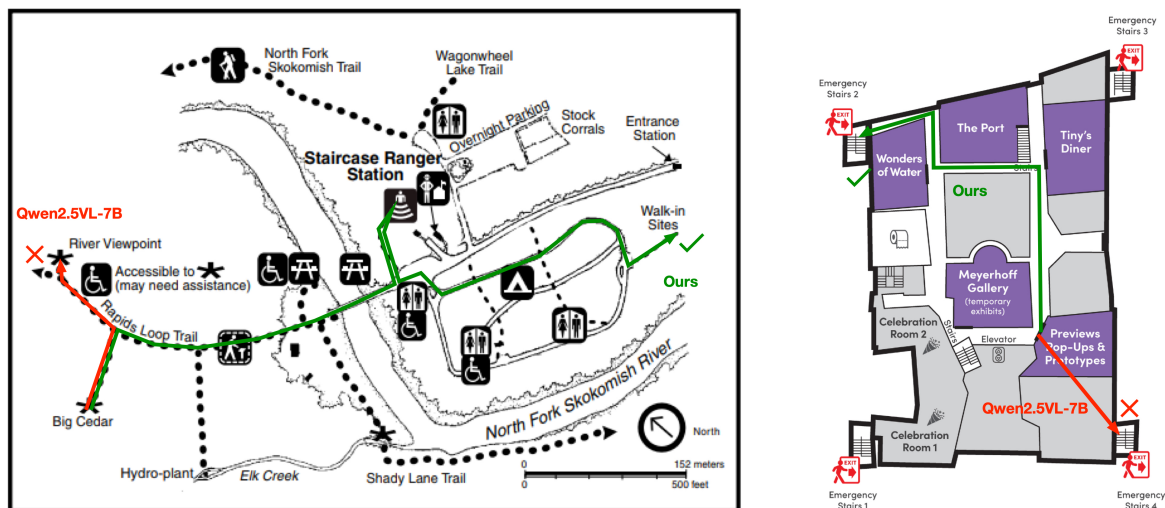


Figure 5 Navigation results on MapBench [10]. **Left:** Trail task with an unstructured outdoor layout. **Right:** Museum task with a structured indoor layout. The baseline Qwen2.5-VL-7B-Instruct model [18] (red) produces incomplete or less feasible trajectories due to issues such as target misidentification, inefficient detours, or violations of environmental constraints. In comparison, Ariadne (green) demonstrates more consistent and goal-directed planning while adhering to structural boundaries.

As shown in Figure 5, the two models exhibit a clear divergence in real-world map-based navigation across diverse task settings. The baseline Qwen2.5-VL-7B-Instruct exhibits localization and planning errors, such as misidentifying targets, taking inefficient detours, or violating environmental constraints like rivers and walls, leading to incomplete or infeasible trajectories. In contrast, Ariadne employs fine-grained, node-level planning that maintains goal-directed navigation while respecting structural boundaries. This behavior generalizes across both unstructured outdoor networks (e.g., trails) and structured indoor layouts (e.g., museums), demonstrating the effectiveness of GRPO adaptations beyond synthetic mazes.

To further assess the transferability of these navigation gains to broader reasoning abilities, we evaluate both models on ReasonMap, a benchmark that probes stepwise reasoning under varying difficulty levels (Figure 6). The dataset includes 55 samples for easy–easy, 46 for easy–middle, 28 for middle–easy, 7 for hard–easy, 23 for middle–middle, 80 for easy–hard, 1 for hard–middle, 57 for middle–hard, and 15 for hard–hard. The first

term indicates question difficulty, while the second term represents map difficulty. The results show that Ariadne achieves consistent gains in long reasoning regimes, particularly in higher-complexity categories such as easy–middle and easy–hard, which correspond to question complexity and map complexity, respectively. For instance, in the easy–hard category, it achieves both a higher average map score (5.17 vs. 4.65) and accuracy (6.67% vs. 5%) compared to the baseline. These improvements are not observed in short reasoning settings, where performance between the two models remains comparable. Overall, the findings suggest that the maze-specific GRPO training paradigm enhances not only real-world navigation robustness but also the model’s capacity for multi-step, long-horizon reasoning, an ability directly relevant to generalizing beyond controlled synthetic tasks.

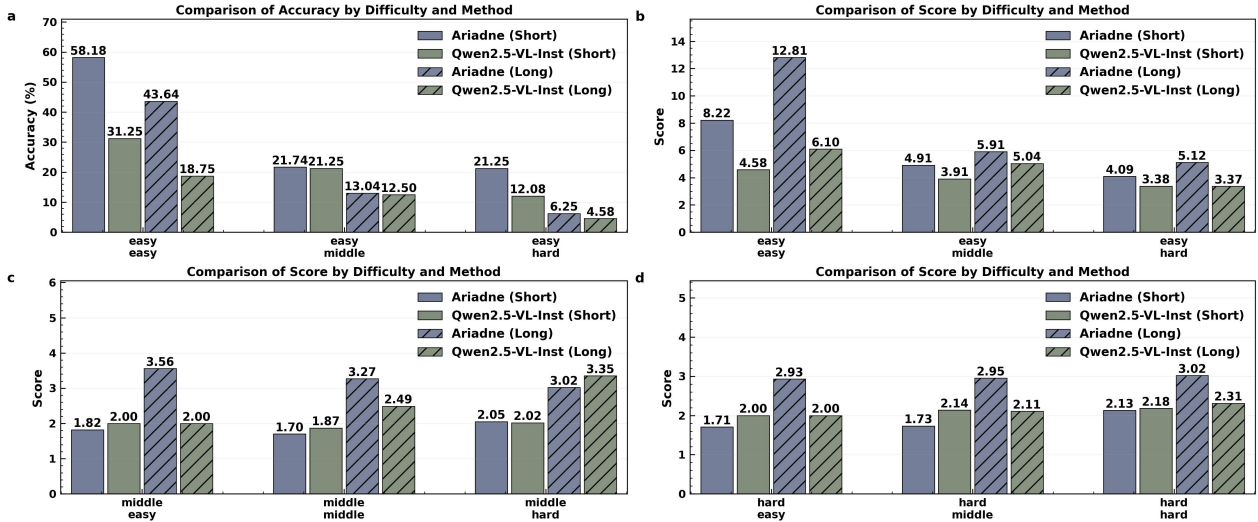


Figure 6 Performance comparison on ReasonMap across varying question and map difficulty levels. (a) Accuracy comparison showing that Ariadne consistently outperforms Qwen2.5-VL-7B-Instruct after GRPO training. (b–d) Average map scores across different combinations of question and map difficulty, illustrating that Ariadne achieves higher scores in most settings, particularly in more complex reasoning categories.

Table 1 Performance comparison on MapBench. **Bold** indicates the best performance.

Model	Google Map ↓	Mall ↓	Museum ↓	National Park ↓	Theme Park ↓	Trail ↓	Campus ↓	Urban ↓	Zoo ↓
Qwen2.5-VL-7B-Instruct	1.61	1.43	1.43	1.86	1.78	2.29	1.62	1.93	1.68
Ariadne	1.30	1.41	1.33	1.48	1.46	1.47	1.29	1.91	1.32

Table 2 Performance comparison on ReasonMap. *S* indicates short questions, *L* indicates long questions. **Bold** indicates the best performance.

Model	Weighted Acc. (<i>S</i>) ↑	#Tokens (<i>S</i>)	Weighted Acc. (<i>L</i>) ↑	#Tokens (<i>L</i>)	Weighted Map Score (<i>S</i> / <i>L</i>) ↑
Qwen2.5-VL-7B-Instruct	13.32%	26	6.00%	61	3.73 / 4.51
Ariadne	14.50%	43	7.47%	121	3.67 / 5.15

Overall, Ariadne achieves strong performance on MapBench and ReasonMap (Tables 1 and 2). The model generalizes well across diverse spatial layouts, from unstructured outdoor networks to structured indoor grids, and demonstrates clear gains in long-horizon, multi-turn reasoning. These improvements are most apparent under high path complexity and extended reasoning chains, where instruction-tuned baselines degrade notably. Together, the results suggest that GRPO training on synthetic maze data effectively enhances spatial-visual reasoning, improving the model’s capability to handle complex real-world tasks.

5 Conclusion

In this work, we introduced Ariadne, a controllable framework for systematically probing and extending the visual reasoning capabilities of VLMs through RLVR. Our experiments demonstrate that RLVR effectively

extends the reasoning boundaries of VLMs, enabling models trained on short and simple trajectories to generalize to longer and more complex cases. Furthermore, the improvements transfer robustly to real-world settings, even under visual domain shifts, indicating that visual reasoning skills acquired in synthetic environments are transferable across diverse visual contexts. However, we observe a sharp decline in performance beyond a critical complexity threshold. This limitation suggests that RLVR may only strengthen and extend reasoning patterns learned during pretraining, rather than inducing entirely new reasoning mechanisms absent from the pretraining data. Future work will explore how controllable reinforcement learning can be integrated into the pretraining stage to further expand the fundamental reasoning capacity of VLMs.

References

- [1] L. Ouyang, J. Wu, X. Jiang, D. Almeida, C. L. Wainwright, P. Mishkin, C. Zhang, S. Agarwal, K. Slama, A. Ray, J. Schulman, J. Hilton, F. Kelton, L. Miller, M. Simens, A. Askell, P. Welinder, P. Christiano, J. Leike, and R. Lowe, “Training language models to follow instructions with human feedback,” in *Proceedings of the International Conference on Neural Information Processing Systems*, 2022.
- [2] J. Schulman, F. Wolski, P. Dhariwal, A. Radford, and O. Klimov, “Proximal policy optimization algorithms,” *arXiv preprint arXiv:1707.06347*, 2017.
- [3] DeepSeek-AI, D. Guo, D. Yang, H. Zhang, J. Song, R. Zhang, R. Xu, Q. Zhu, S. Ma, P. Wang, X. Bi, X. Zhang, X. Yu, Y. Wu, Z. F. Wu, Z. Gou, Z. Shao, Z. Li, Z. Gao, A. Liu, B. Xue, B. Wang, B. Wu, B. Feng, C. Lu, C. Zhao, C. Deng, C. Zhang, C. Ruan, D. Dai, D. Chen, D. Ji, E. Li, F. Lin, F. Dai, F. Luo, G. Hao, G. Chen, G. Li, H. Zhang, H. Bao, H. Xu, H. Wang, H. Ding, H. Xin, H. Gao, H. Qu, H. Li, J. Guo, J. Li, J. Wang, J. Chen, J. Yuan, J. Qiu, J. Li, J. L. Cai, J. Ni, J. Liang, J. Chen, K. Dong, K. Hu, K. Gao, K. Guan, K. Huang, K. Yu, L. Wang, L. Zhang, L. Zhao, L. Wang, L. Zhang, L. Xu, L. Xia, M. Zhang, M. Zhang, M. Tang, M. Li, M. Wang, M. Li, N. Tian, P. Huang, P. Zhang, Q. Wang, Q. Chen, Q. Du, R. Ge, R. Zhang, R. Pan, R. Wang, R. J. Chen, R. L. Jin, R. Chen, S. Lu, S. Zhou, S. Chen, S. Ye, S. Wang, S. Yu, S. Zhou, S. Pan, and S. S. Li, “Deepseek-r1: Incentivizing reasoning capability in llms via reinforcement learning,” *arXiv preprint arXiv:2501.12948*, 2025.
- [4] Z. Shao, P. Wang, Q. Zhu, R. Xu, J. Song, X. Bi, H. Zhang, M. Zhang, Y. Li, Y. Wu *et al.*, “Deepseekmath: Pushing the limits of mathematical reasoning in open language models,” *arXiv preprint arXiv:2402.03300*, 2024.
- [5] W. Huang, B. Jia, Z. Zhai, S. Cao, Z. Ye, F. Zhao, Z. Xu, Y. Hu, and S. Lin, “Vision-r1: Incentivizing reasoning capability in multimodal large language models,” *arXiv preprint arXiv:2503.06749*, 2025.
- [6] H. Wang, C. Qu, Z. Huang, W. Chu, F. Lin, and W. Chen, “Vl-rethinker: Incentivizing self-reflection of vision-language models with reinforcement learning,” *arXiv preprint arXiv:2504.08837*, 2025.
- [7] Z. Wan, Z. Dou, C. Liu, Y. Zhang, D. Cui, Q. Zhao, H. Shen, J. Xiong, Y. Xin, Y. Jiang *et al.*, “Srpo: Enhancing multimodal llm reasoning via reflection-aware reinforcement learning,” *arXiv preprint arXiv:2506.01713*, 2025.
- [8] A. Dao and D. B. Vu, “Alphamaze: Enhancing large language models’ spatial intelligence via grp0,” *arXiv preprint arXiv:2502.14669*, 2025.
- [9] P. Mirowski, R. Pascanu, F. Viola, H. Soyer, A. Ballard, A. Banino, M. Denil, R. Goroshin, L. Sifre, K. Kavukcuoglu, D. Kumaran, and R. Hadsell, “Learning to navigate in complex environments,” in *Proceedings of International Conference on Learning Representations*, 2017.
- [10] S. Xing, Z. Sun, S. Xie, K. Chen, Y. Huang, Y. Wang, J. Li, D. Song, and Z. Tu, “Can large vision language models read maps like a human?” *arXiv preprint arXiv:2503.14607*, 2025.
- [11] S. Feng, S. Wang, S. Ouyang, L. Kong, Z. Song, J. Zhu, H. Wang, and X. Wang, “Can mllms guide me home? a benchmark study on fine-grained visual reasoning from transit maps,” *arXiv preprint arXiv:2505.18675*, 2025.
- [12] J.-B. Alayrac, J. Donahue, P. Luc, A. Miech, I. Barr, Y. Hasson, K. Lenc, A. Mensch, K. Millican, M. Reynolds, R. Ring, E. Rutherford, S. Cabi, T. Han, Z. Gong, S. Samangooei, M. Monteiro, J. Menick, S. Borgeaud, A. Brock, A. Nematzadeh, S. Sharifzadeh, M. Binkowski, R. Barreira, O. Vinyals, A. Zisserman, and K. Simonyan, “Flamingo: a visual language model for few-shot learning,” in *Proceedings of Advances in Neural Information Processing Systems*, 2022.
- [13] H. Liu, C. Li, Q. Wu, and Y. J. Lee, “Visual instruction tuning,” in *Proceedings of Conference on Neural Information Processing Systems*, 2023.
- [14] J. Zhu, W. Wang, Z. Chen, Z. Liu, S. Ye, L. Gu, H. Tian, Y. Duan, W. Su, J. Shao *et al.*, “Internvl3: Exploring advanced training and test-time recipes for open-source multimodal models,” *arXiv preprint arXiv:2504.10479*, 2025.
- [15] J. Wei, X. Wang, D. Schuurmans, M. Bosma, brian ichter, F. Xia, E. H. Chi, Q. V. Le, and D. Zhou, “Chain of thought prompting elicits reasoning in large language models,” in *Proceedings of Advances in Neural Information Processing Systems*, 2022.
- [16] B. Ji, S. Agrawal, Q. Tang, and Y. Wu, “Enhancing spatial reasoning in vision-language models via chain-of-thought prompting and reinforcement learning,” *arXiv preprint arXiv:2507.13362*, 2025.
- [17] Q. Zhao, Y. Lu, M. J. Kim, Z. Fu, Z. Zhang, Y. Wu, Z. Li, Q. Ma, S. Han, C. Finn *et al.*, “Cot-vla: Visual chain-of-thought reasoning for vision-language-action models,” in *Proceedings of the Computer Vision and Pattern Recognition Conference*, 2025, pp. 1702–1713.
- [18] S. Bai, K. Chen, X. Liu, J. Wang, W. Ge, S. Song, K. Dang, P. Wang, S. Wang, J. Tang, H. Zhong, Y. Zhu, M. Yang, Z. Li, J. Wan, P. Wang, W. Ding, Z. Fu, Y. Xu, J. Ye, X. Zhang, T. Xie, Z. Cheng, H. Zhang, Z. Yang, H. Xu, and J. Lin, “Qwen2.5-vl technical report,” *arXiv preprint arXiv:2502.13923*, 2025.